

Directions of Motion Fields Are Hardly Ever Ambiguous

Tomas Brodsky, Cornelia Fermüller, and Yiannis Aloimonos

Computer Vision Laboratory, Center for Automation Research, Dept. of Computer
Science and Institute of Advanced Computer Studies, University of Maryland,
College Park, MD 20742-3275

Abstract. Recent literature [7, 10, 11, 9, 13, 17] provides a number of results regarding uniqueness aspects of motion fields and exact image displacements due to 3-D rigid motion. Here instead of the full motion field we consider only the direction of the motion field due to a rigid motion and ask what can we say about the three-dimensional motion information contained in it. This paper provides a geometric analysis of this question based solely on the fact that the depth of the surfaces in view is positive (i.e. that the surface in view is in front of the camera). With this analysis we thus offer a theoretical foundation for image constraints employing only the sign of flow in various directions and provide a solid basis for their utilization in addressing 3D dynamic vision problems.

For two different rigid motions (with instantaneous translational and rotational velocities (t_1, ω_1) and (t_2, ω_2)) to yield the same direction of the flow, the surfaces in view must satisfy certain inequality and equality constraints, called critical surface constraints. A complete description of image areas where the constraints cannot be satisfied is derived and it is shown that if the imaging surface is a whole sphere, any two motions with different translation and rotation axes can be distinguished using only the direction of the flow. In the case where the imaging surface is a hemisphere or a plane, it is shown that two motions could give rise to the same direction of the flow if $(t_1 \times t_2) \cdot (\omega_1 \times \omega_2) = 0$ and several additional constraints are satisfied. For this to occur, the surfaces in view must satisfy all the critical surface constraints; thus at some points only a single depth value is allowed. Similar results are obtained for the case of multiple motions. Consequently, directions of motion fields are hardly ever ambiguous.

1 Introduction and Motivation

The basis of the majority of visual motion studies has been the motion field, i.e., the projection of the velocities of 3D scene points on the image. Classical

The support of the Advanced Research Projects Agency (ARPA Order No. 8459) and the U.S. Army Topographic Engineering Center under Contract DACA76-92-C-0009, the Office of Naval Research under Contract N00014-93-1-0257, National Science Foundation under Grant IRI-90-57934, , and the Austrian “Fonds zur Förderung der wissenschaftlichen Forschung”, project No. S 7003, is gratefully acknowledged.

results on the uniqueness of motion fields [7, 10, 11] as well as displacement fields [9, 13, 17] have formed the foundation of most research on rigid motion analysis that addressed the 3D motion problem by first approximating the motion field through the optical flow and then interpreting the optical flow to obtain 3D motion and structure [15, 8, 16, 18, 14].

The difficulties involved in the estimation of optical flow have recently given rise to a small number of studies considering as input to the visual motion interpretation process some partial optical flow information. In particular the projection of the optical flow on the gradient direction, the so-called normal flow [6, 12], and the projections of the flow on different directions [1, 3, 4] have been utilized. In [3] constraints on the sign of the projection of the flow on various directions were presented. These constraints on the sign of the flow were derived using only the rigid motion model, with the only constraint on the scene being that the depth in view has to be positive at every point—the so-called “depth-positivity” constraint. In the sequel we are led naturally to the question of what these constraints, or more generally any constraint on the sign of the flow, can possibly tell us about three-dimensional motion and the structure of the scene in view. Thus we would like to investigate the amount of information in the sign of the projection of the flow. Since knowing the sign of the projection of a motion vector in all directions is equivalent to knowing the direction of the motion vector, our question amounts to studying the relationship between the directions of 2D motion vectors and 3D rigid motion.

The 2D motion field on the imaging surface is the projection of the 3D motion field of the scene points moving relative to that surface. We use a coordinate system $OXYZ$ fixed to the camera. The center of projection is at the origin and the image is formed on a sphere with radius 1. A scene point \mathbf{R} is projected onto an image point $\mathbf{r} = \mathbf{R}/|\mathbf{R}|$, where $|\mathbf{R}|$ is the norm of the vector \mathbf{R} .

Suppose the observer is moving rigidly with instantaneous translation $\mathbf{t} = (U, V, W)$ and instantaneous rotation $\boldsymbol{\omega} = (\alpha, \beta, \gamma)$. The well-known equation for the motion field at point \mathbf{r} is

$$\dot{\mathbf{r}} = v_{\text{tr}}(\mathbf{r}) + v_{\text{rot}}(\mathbf{r}) = \frac{1}{|\mathbf{R}|}((\mathbf{t} \cdot \mathbf{r})\mathbf{r} - \mathbf{t}) - \boldsymbol{\omega} \times \mathbf{r} = -\frac{1}{|\mathbf{R}|}(\mathbf{r} \times (\mathbf{t} \times \mathbf{r})) - \boldsymbol{\omega} \times \mathbf{r} .$$

The first term $v_{\text{tr}}(\mathbf{r})$ corresponds to the translational component which depends on the depth $Z = |\mathbf{R}|$, the distance of \mathbf{R} to the center of projection. The direction of $v_{\text{tr}}(\mathbf{r})$ is along great circles (longitudes) pointing away from the Focus of Expansion (\mathbf{t}) and towards the Focus of Contraction ($-\mathbf{t}$). The second term $v_{\text{rot}}(\mathbf{r})$ corresponds to the rotational component which is independent of depth. Its direction is along latitudes around the axis of rotation (counterclockwise around $\boldsymbol{\omega}$ and clockwise around $-\boldsymbol{\omega}$).

As can be seen, even from exact optical flow, without additional constraints there is an ambiguity in the computation of shape and translation. It is not possible to disentangle the effects of \mathbf{t} and $|\mathbf{R}|$, and thus we can only derive the direction of translation. If we only consider the sign of optical flow, in addition we are also restricted in the computation of the rotational parameters. If we

multiply ω by a positive constant, leave \mathbf{t} fixed, but multiply $\frac{1}{|\mathbf{R}|}$ by the same positive constant, the sign of the flow is not affected. Thus from the direction of the flow we can at most compute the axis of rotation and, as discussed before, the axis of translation.

Hereafter, for the sake of brevity, we will refer to the motion field also as the flow field or simply flow, and to the direction of the motion field as the directional flow field or simply directional flow.

In this paper, by pursuing a theoretical investigation of the amount of information present in directional flow fields, we demonstrate the power of the qualitative image measurements already used empirically, and justify their utilization in global constraints for three-dimensional dynamic vision problems. We study here the theoretical question, investigating uniqueness issues in a noise-free flow field. In practical situations, of course, inaccurate estimation of image displacement directions might influence the result of 3D motion estimation, but this is not the issue we are concerned with here.

The organization of this paper is as follows: In Sect. 2 we develop the preliminaries: Given two rigid motions, we study what the constraints are on the surfaces in view for the two motion fields to have the same direction at every point. In Sect. 3, using these constraints, we study conditions under which two rigid flow fields could have the same direction at every point on a hemisphere. In Sect. 4, we investigate the ambiguity of multiple motions. Section 5 summarizes the results.

2 Critical Surface Constraints

Let us assume that two different rigid motions (\mathbf{t}_1, ω_1) and (\mathbf{t}_2, ω_2) yield the same directional flow at every point in the image. To simplify the explanations, we assume $\mathbf{t}_1 \times \mathbf{t}_2 \neq 0$ and $\omega_1 \times \omega_2 \neq 0$. The special cases are dealt with in Sect. 3.3.

Since from the direction of flow we can only recover the directions of the translation and rotation axes, we assume all four vectors \mathbf{t}_1 , \mathbf{t}_2 , ω_1 and ω_2 to be of unit length. Let $Z_1(\mathbf{r})$ and $Z_2(\mathbf{r})$ be the functions, mapping points \mathbf{r} on the image into the real numbers, that represent the depths of the surfaces in view corresponding to the two motions. In the future we will refer to Z_1 and Z_2 as the two depth maps. We assume that the two depths are positive, and allow Z_1 or Z_2 to be infinitely large. Thus we assume $1/Z_1 \geq 0$ and $1/Z_2 \geq 0$.

2.1 Notation

We denote $f_\omega(\mathbf{r}) = [\omega_1 \ \omega_2 \ \mathbf{r}]$, $f_t(\mathbf{r}) = [\mathbf{t}_1 \ \mathbf{t}_2 \ \mathbf{r}]$, and $g_{ij}(\mathbf{r}) = (\omega_i \times \mathbf{r}) \cdot (\mathbf{t}_j \times \mathbf{r})$, where $[\mathbf{abc}] = (\mathbf{a} \times \mathbf{b}) \cdot \mathbf{c}$ denotes the triple product of vectors \mathbf{a} , \mathbf{b} and \mathbf{c} .

These functions have a simple geometric meaning. Function $f_\omega(\mathbf{r})$ is zero for points \mathbf{r} lying on a geodesic passing through ω_1 and ω_2 . The geodesic is the locus of points \mathbf{r} where $v_{\text{rot}_1}(\mathbf{r})$, the rotational component of the first motion, is parallel to $v_{\text{rot}_2}(\mathbf{r})$, the rotational component of the second motion. Similarly,

the geodesic passing through \mathbf{t}_1 and \mathbf{t}_2 is the locus of points where $f_t(\mathbf{r}) = 0$ and $v_{tr_1}(\mathbf{r})$ is parallel to $v_{tr_2}(\mathbf{r})$.

Equation $g_{ij}(\mathbf{r}) = 0$ defines a second order contour consisting of two closed curves on the sphere, the so-called zero motion contour of motion $(\mathbf{t}_j, \boldsymbol{\omega}_i)$ (see Fig. 1). It is the locus of points where $v_{rot_i}(\mathbf{r})$ is parallel to $v_{tr_j}(\mathbf{r})$, and therefore the locus of points where the flow due to the motion $(\mathbf{t}_j, \boldsymbol{\omega}_i)$ could be zero. Throughout the paper the functions $f_i(\mathbf{r})$, $g_{ij}(\mathbf{r})$ and the curves defined by their zero crossings will play very important roles.

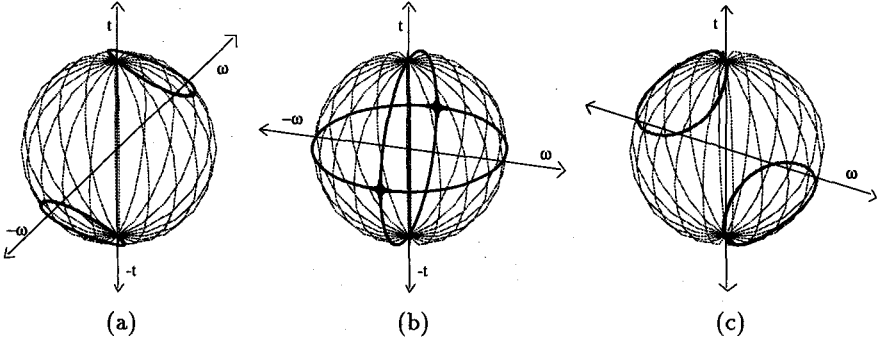


Fig. 1. The zero motion contour (the locus of points \mathbf{r} where $\dot{\mathbf{r}}$ could be zero) consists of two closed curves on the sphere. Three possible configurations are (a) $(\boldsymbol{\omega} \cdot \mathbf{t}) > 0$, (b) $(\boldsymbol{\omega} \cdot \mathbf{t}) = 0$, and (c) $(\boldsymbol{\omega} \cdot \mathbf{t}) < 0$.

To simplify the notation we will usually drop \mathbf{r} and write only f_i and g_{ij} where the index i in f_i can take values t and ω . By simple vector manipulation, we can prove a useful relationship between f_i and g_{ij}

$$g_{11}g_{22} = f_t f_\omega + g_{12}g_{21} \quad (1)$$

2.2 Conditions for Ambiguity

The two motions can give rise to the same directional flow fields if at any point \mathbf{r} there exists $\mu > 0$ such that

$$-\frac{1}{Z_1}(\mathbf{r} \times (\mathbf{t}_1 \times \mathbf{r})) - \boldsymbol{\omega}_1 \times \mathbf{r} = \mu \left(-\frac{1}{Z_2}(\mathbf{r} \times (\mathbf{t}_2 \times \mathbf{r})) - \boldsymbol{\omega}_2 \times \mathbf{r} \right) \quad (2)$$

Projecting the vector equation (2) on directions $\mathbf{t}_2 \times \mathbf{r}$ and $\mathbf{r} \times (\boldsymbol{\omega}_2 \times \mathbf{r})$ and using $\mu > 0$, we obtain two constraints for Z_1 :

$$\text{sgn}\left(\frac{1}{Z_1} f_t + g_{12}\right) = \text{sgn}(g_{22}) \quad (3)$$

$$\text{sgn}\left(\frac{1}{Z_1} g_{21} - f_\omega\right) = \text{sgn}\left(\frac{1}{Z_2} g_{22}\right) \quad (4)$$

where $\text{sgn}(\cdot)$ denotes the sign function.

We define $s_1 = -g_{12}/f_t$ and $s'_1 = f_\omega/g_{21}$. At any point, f_i and g_{ij} are constant, so (3) and (4) provide simple constraints on $1/Z_1$. We call them the s_1 -constraint and the s'_1 -constraint respectively.

We see that the depth Z_1 has a relationship to the surfaces $1/s_1(\mathbf{r})$ and $1/s'_1(\mathbf{r})$. To express the surfaces in scene coordinates \mathbf{R} , we substitute in the above equations $Z(\mathbf{r})\mathbf{r} = \mathbf{R}$ and obtain

$$(\mathbf{t}_1 \times \mathbf{t}_2) \cdot \mathbf{R} + (\boldsymbol{\omega}_1 \times \mathbf{R}) \cdot (\mathbf{t}_2 \times \mathbf{R}) = 0 \quad (5)$$

$$\text{and} \quad (\boldsymbol{\omega}_2 \times \mathbf{R}) \cdot (\mathbf{t}_1 \times \mathbf{R}) - ((\boldsymbol{\omega}_1 \times \boldsymbol{\omega}_2) \cdot \mathbf{R})\mathbf{R}^2 = 0 \quad (6)$$

Thus Z_1 is constrained by a second order surface through (5) and by a third order surface through (6). At some points it has to be inside the first surface and at some points it has to be outside the first surface. In addition, at some points it has to be inside the second surface and at some points it has to be outside the second surface. Figure 2 provides a pictorial description of the two surfaces constraining Z_1 .

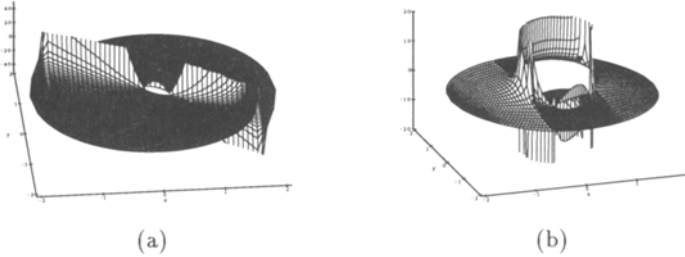


Fig. 2. Two rigid motions $(\mathbf{t}_1, \boldsymbol{\omega}_1)$, $(\mathbf{t}_2, \boldsymbol{\omega}_2)$ constrain the possible depth Z_1 of the first surface by a second and a third order surface. The particular surfaces shown in the coordinate system of the imaging sphere, projected stereographically, correspond to the motion configuration of Fig. 3.

We can repeat the above derivation for the depth map Z_2 . Projecting (2) on vectors $\mathbf{t}_1 \times \mathbf{r}$ and $\mathbf{r} \times (\boldsymbol{\omega}_1 \times \mathbf{r})$, we obtain

$$\text{sgn}(g_{11}) = \text{sgn}\left(-\frac{1}{Z_2}f_t + g_{21}\right) \quad (7)$$

$$\text{sgn}\left(\frac{1}{Z_1}g_{11}\right) = \text{sgn}\left(\frac{1}{Z_2}g_{12} + f_\omega\right) \quad (8)$$

We define $s_2 = g_{21}/f_t$, $s'_2 = -f_\omega/g_{12}$. Equations (7) and (8) provide constraints on $1/Z_2$, and we thus call them the s_2 -constraint and the s'_2 -constraint.

2.3 Interpretation of Surface Constraints

At each point we have a s_1 -constraint (depending on signs of f_t , g_{12} , and g_{22}), a s'_1 -constraint (depending on signs of g_{21} , f_ω , and g_{22}), and an additional constraint $1/Z_1 \geq 0$. If the constraints cannot be satisfied, the two flows at this point cannot have the same direction and we say that we have a *contradictory point*.

The existence of a solution for $1/Z_1$ depends also on the sign of $s_1 - s'_1$. Using (1), we can write $s_1 - s'_1 = -(g_{11} g_{22}) / (f_t g_{21})$. So we see that $\text{sgn}(s_1 - s'_1)$ can change only at points where at least one of f_i , g_{ij} is zero.

At points where $g_{22} = 0$ we have the s_1 -constraint $1/Z_1 = s_1$, the s'_1 -constraint $1/Z_1 = s'_1$, and also $s_1 = s'_1$; thus at these points there is a unique value of Z_1 satisfying the constraints.

The analysis for Z_2 yields the same results. In summary, the curves $f_i(\mathbf{r}) = 0$ and $g_{ij}(\mathbf{r}) = 0$ separate the sphere into a number of areas. Each of the areas is either contradictory (i.e., containing only contradictory points), or ambiguous (i.e., containing points where the two motion vectors can have the same direction). Two different rigid motions can produce ambiguous directions of flow if the image contains only points from ambiguous areas. There are also two scene surfaces constraining depth Z_1 and two surfaces constraining depth Z_2 . If the depths do not satisfy the constraints, the two flows are not ambiguous.

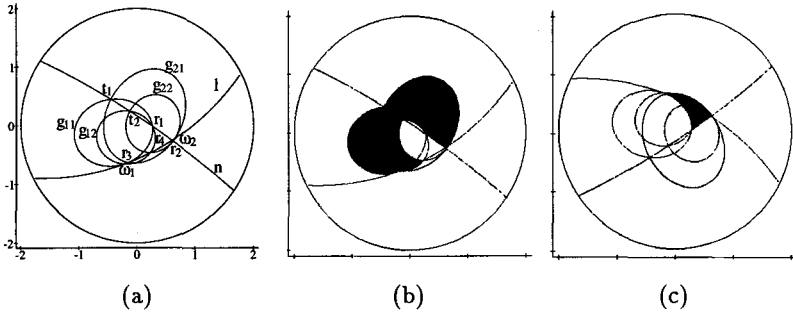


Fig. 3. (a) Separation of the sphere through curves $f_i = 0$ and $g_{ij} = 0$. (b), (c) Contradictory areas for both halves of the sphere.

2.4 Contradictory Points

Since we are interested in contradictory areas, we investigate only a general case, i.e. assume $f_i \neq 0$ and $g_{ij} \neq 0$. Special cases are discussed separately.

If $1/Z_1 < s_1 < 0$, or $1/Z_1 \leq s'_1 < 0$, there is no solution for Z_1 . This happens under conditions C_1 and C_2 :

$$\text{sgn}(f_t) = \text{sgn}(g_{12}) = -\text{sgn}(g_{22}) \quad (9)$$

$$\operatorname{sgn}(f_\omega) = -\operatorname{sgn}(g_{21}) = \operatorname{sgn}(g_{22}) \quad (10)$$

The similar conditions C_3 and C_4 for Z_2 are

$$\operatorname{sgn}(f_t) = -\operatorname{sgn}(g_{21}) = \operatorname{sgn}(g_{11}) \quad (11)$$

$$\operatorname{sgn}(f_\omega) = \operatorname{sgn}(g_{12}) = -\operatorname{sgn}(g_{11}) \quad (12)$$

We call these four constraints (C_1 – C_4) Contradictory Point conditions, or CP-conditions for short. We can show that a point (where $f_i \neq 0$ and $g_{ij} \neq 0$) is contradictory if and only if at least one of the four conditions is satisfied.

2.5 Antipodal Pairs of Points

Let us now consider point \mathbf{r} and its antipodal point $-\mathbf{r}$ such that $f_i(\mathbf{r}) \neq 0$ and $g_{ij}(\mathbf{r}) \neq 0$. Clearly, $f_i(-\mathbf{r}) = -f_i(\mathbf{r})$, but $g_{ij}(-\mathbf{r}) = g_{ij}(\mathbf{r})$.

Both point \mathbf{r} and point $-\mathbf{r}$ are ambiguous only if the CP-conditions are not satisfied. This occurs when

$$\operatorname{sgn}(g_{11}(\mathbf{r})) = \operatorname{sgn}(g_{12}(\mathbf{r})) = \operatorname{sgn}(g_{21}(\mathbf{r})) = \operatorname{sgn}(g_{22}(\mathbf{r})) \quad (13)$$

Let the imaging surface be a whole sphere. The two motions are different, thus there always exist areas on the sphere where condition (13) is not satisfied. Since for any point the image contains also its antipodal point, clearly some areas in the image are contradictory.

3 The Geometry of the Depth-Positivity Constraint

In the previous section we have shown that any two rigid motions can be distinguished using directional flow if the image is a whole sphere. From now on, we assume that the image is a half of the sphere. Let the image hemisphere be bounded by equator q and let \mathbf{n}_0 be a unit vector normal to the plane of q such that point \mathbf{n}_0 lies in the image.

3.1 Half Sphere Image: The General Case

Let us assume that $(\boldsymbol{\omega}_1 \times \boldsymbol{\omega}_2) \cdot (\mathbf{t}_1 \times \mathbf{t}_2) \neq 0$. We show that under this condition the two rigid motions cannot produce motion fields with the same direction everywhere in the image.

We project point $\boldsymbol{\omega}_1$ on the geodesic n connecting \mathbf{t}_1 and \mathbf{t}_2 to obtain point $\mathbf{r}_1 = (\mathbf{t}_1 \times \mathbf{t}_2) \times (\boldsymbol{\omega}_1 \times (\mathbf{t}_1 \times \mathbf{t}_2))$. It can be shown that point \mathbf{r}_1 is always contradictory and also one of the areas around \mathbf{r}_1 is contradictory, because (12) or (11) is satisfied.

Just as we projected $\boldsymbol{\omega}_1$ on geodesic n connecting \mathbf{t}_1 and \mathbf{t}_2 to obtain \mathbf{r}_1 , we project $\boldsymbol{\omega}_2$ on n to obtain \mathbf{r}_2 , and we project \mathbf{t}_1 and \mathbf{t}_2 on geodesic l , connecting $\boldsymbol{\omega}_1$ and $\boldsymbol{\omega}_2$, to obtain \mathbf{r}_3 and \mathbf{r}_4 (see Fig. 3). Again, each of \mathbf{r}_i (and one of its neighboring areas) is contradictory, since one of the CP-constraints must be valid.

3.2 Half Sphere Image: The Ambiguous Case

We now consider the case $(\mathbf{t}_1 \times \mathbf{t}_2) \cdot (\boldsymbol{\omega}_1 \times \boldsymbol{\omega}_2) = 0$. However, we still assume $\mathbf{t}_1 \times \mathbf{t}_2 \neq 0$ and $\boldsymbol{\omega}_1 \times \boldsymbol{\omega}_2 \neq 0$. Then contour $f_t = 0$ is perpendicular to $f_\omega = 0$, and $\mathbf{r}_1 = \mathbf{r}_2 = \mathbf{r}_3 = \mathbf{r}_4$.

The motions can be ambiguous only if contours g_{ij} do not intersect the equator q (because of (13)). We obtain a condition

$$l = [\mathbf{t}_j \boldsymbol{\omega}_i \mathbf{n}_0]^2 - 4(\boldsymbol{\omega}_i \cdot \mathbf{n}_0)(\mathbf{t}_j \cdot \mathbf{n}_0)(\boldsymbol{\omega}_i \cdot \mathbf{t}_j) < 0. \quad (14)$$

By considering all the possible sign combinations for terms f_i and g_{ij} around \mathbf{r}_1 , it can be verified that the motions are contradictory unless

$$\text{sgn}(\mathbf{t}_1 \cdot \mathbf{n}_0) = \text{sgn}(\mathbf{t}_2 \cdot \mathbf{n}_0) \quad (15)$$

$$\text{sgn}(\boldsymbol{\omega}_1 \cdot \mathbf{n}_0) = \text{sgn}(\boldsymbol{\omega}_2 \cdot \mathbf{n}_0) \quad (16)$$

$$\text{sgn}(((\boldsymbol{\omega}_1 \times \boldsymbol{\omega}_2) \times (\mathbf{t}_1 \times \mathbf{t}_2)) \cdot \mathbf{n}_0) = \text{sgn}(\mathbf{t}_1 \cdot \mathbf{n}_0) \text{sgn}(\boldsymbol{\omega}_1 \cdot \mathbf{n}_0) \quad (17)$$

In summary, two rigid motions can be ambiguous on one hemisphere if vector $(\mathbf{t}_1 \times \mathbf{t}_2)$ is perpendicular to vector $(\boldsymbol{\omega}_1 \times \boldsymbol{\omega}_2)$ and all conditions (14), (15), (16), and (17) are satisfied. In addition, as shown in Sect. 2, the two surfaces in view are constrained by a second and a third order surface. Figure 4 gives an example of such a contradictory configuration.

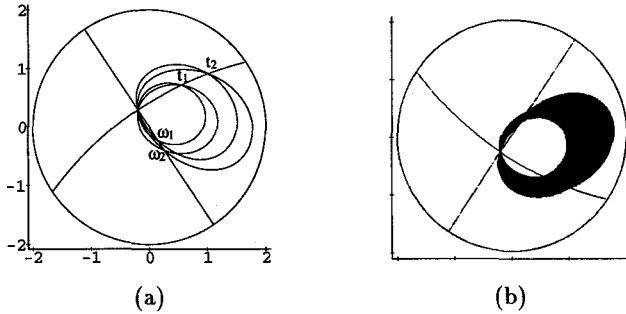


Fig. 4. Both halves of the sphere showing two rigid motions for which there do not exist contradictory areas in one hemisphere. (a) Hemisphere containing only ambiguous areas. (b) Contradictory areas on the other hemisphere.

3.3 Special Cases

For the special cases it can be shown that if $\mathbf{t}_1 \times \mathbf{t}_2 = 0$ or $\boldsymbol{\omega}_1 \times \boldsymbol{\omega}_2 = 0$, ambiguity cannot occur. A detailed analysis is given in [2].

4 Ambiguity of More than Two Motions

In [2], the analysis has been extended to multiple 3-D motions. Considering three rigid motions, conditions similar to the CP-conditions have been developed. Checking their validity at the intersections of the various zero-motion contours and geodesics through the points t_i and ω_i , it has been shown that three or more rigid motions (t_i, ω_i) could give rise to the same directional flow only if all the t_i lie on a geodesic n and all the ω_i lie on a geodesic l perpendicular to n . Also, all the zero-motion contours $g_{ii} = 0$ must intersect in the same points. For an illustration see Fig. 5.

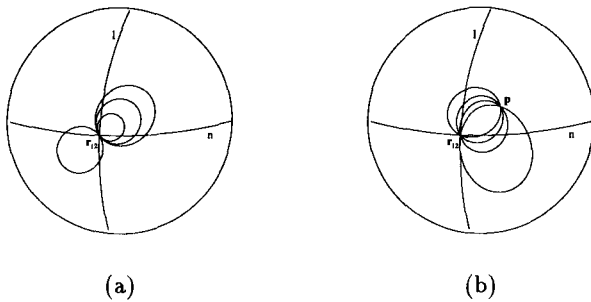


Fig. 5. Two possible configurations of multiple ambiguous motions. (a) All the zero motion contours are tangent at point r_{12} . (b) All the zero motion contours cross at one point $p \neq r_{12}$. There can be an additional ambiguous motion with a degenerate zero-motion contour containing only point p .

5 Conclusions

In this paper we have analyzed the amount of information inherent in the directions of rigid flow fields. We have shown that in almost all cases there is enough information to determine up to a multiplicative constant both the 3D-rotational and 3D-translational motion from a hemispherical image. Ambiguities can result only if the surfaces in view satisfy certain inequality and equality constraints. Furthermore, for two 3D motions to be compatible the two translation vectors must lie on a geodesic perpendicular to the geodesic through the two rotation vectors. With this analysis we have also shown that visual motion analysis does not necessarily require the intermediate computation of optical flow or exact correspondence. Instead, many dynamic vision problems might be solved with the use of more qualitative (and thus robust) flow estimates if appropriate global constraints are found.

References

1. N. Ancona and T. Poggio. Optical flow from 1-D correlation: Application to a simple time-to-crash detector. *International Journal of Computer Vision: Special Issue on Qualitative Vision*, Y. Aloimonos (Ed.), 14:131–146, 1995.
2. T. Brodsky, C. Fermüller and Y. Aloimonos. Directions of motion fields are hardly ever ambiguous. Technical Report CAR-TR-780, Center for Automation Research, University of Maryland, 1995.
3. C. Fermüller. Passive navigation as a pattern recognition problem. *International Journal of Computer Vision: Special Issue on Qualitative Vision*, Y. Aloimonos (Ed.), 14:147–158, 1995.
4. C. Fermüller and Y. Aloimonos. Direct Perception of Three-Dimensional Motion from Patterns of Visual Motion. *Science*, 270:1973–1976, 1995.
5. C. Fermüller and Y. Aloimonos. On the geometry of visual correspondence. *International Journal of Computer Vision*, 1995. To appear.
6. C. Fermüller and Y. Aloimonos. Qualitative egomotion. *International Journal of Computer Vision*, 15:7–29, 1995.
7. B. Horn. Motion fields are hardly ever ambiguous. *International Journal of Computer Vision*, 1:259–274, 1987.
8. B. Horn. Relative orientation. *International Journal of Computer Vision*, 4:59–78, 1990.
9. H. Longuet-Higgins. A computer algorithm for reconstruction of a scene from two projections. *Nature*, 293:133–135, 1981.
10. S. Maybank. *Theory of Reconstruction from Image Motion*. Springer, Berlin, 1993.
11. S. Negahdaripour. Critical surface pairs and triplets. *International Journal of Computer Vision*, 3:293–312, 1989.
12. S. Negahdaripour and B. Horn. Direct passive navigation. *IEEE Transactions on Pattern Analysis and Machine Intelligence*, 9:163–176, 1987.
13. M. Spetsakis and J. Aloimonos. Structure from motion using line correspondences. *International Journal of Computer Vision*, 1:171–183, 1990.
14. M. Spetsakis and J. Aloimonos. A unified theory of structure from motion. In *Proc. ARPA Image Understanding Workshop*, Pittsburgh, PA, pages 271–283, 1990.
15. M. Spetsakis and J. Aloimonos. Optimal Visual Motion Estimation. *IEEE Transactions on PAMI*, 14:959–964, 1992.
16. M. Tistarelli and G. Sandini. Dynamic aspects in active vision. *CVGIP: Image Understanding: Special Issue on Purposive, Qualitative, Active Vision*, Y. Aloimonos (Ed.), 56:108–129, 1992.
17. R. Tsai and T. Huang. Uniqueness and estimation of three-dimensional motion parameters of rigid objects with curved surfaces. *IEEE Transactions on Pattern Analysis and Machine Intelligence*, 6:13–27, 1984.
18. T. Vieville and O. D. Faugeras. Robust and fast computation of edge characteristics in image sequences. *International Journal of Computer Vision*, 13:153–179, 1994.